

MODELING THE EFFECT OF RISING SEA LEVEL ON RIVER DELTAS AND LONG PROFILES OF RIVERS

Gary Parker, Yoshihisa Akamatsu

St. Anthony Falls Laboratory, University of Minnesota
Mississippi River at 3rd Ave. SE, Minneapolis, MN 55414 USA

Tetsuji Muto

Sedimentary Geoscience Laboratory, Faculty of Environmental Sciences
Nagasaki University, 1-14 Bunkyo-machi, Nagasaki 852-8521, Japan

William Dietrich

Department of Earth and Planetary Science, University of California
Berkeley, CA 94720-4767 USA

ABSTRACT

A consequence of the current global warming is rising sea level as polar ice melts. The future effect of such sea level rise on shorelines, river deltas and river long profiles is not well known. The problem may be understood by studying the consequences of Holocene sea level rise after the last glaciation. The melting of the Pleistocene glaciers caused a sea level rise of ~ 120 m, mostly in a period of 12,000 years. Here the effect of rising sea level on river deltas and long profiles is explored numerically for the Fly-Strickland River System, Papua New Guinea. The results suggest that the effect has been felt far upstream from the Pleistocene river delta, creating an embayment and moving the gravel-sand transition upstream.

Keywords: sea level rise, river delta, long profile

INTRODUCTION

Holocene sea level rise and river deltas

The last deglaciation resulted in a global sea level rise of some 120 m. Nearly all this rise was realized in a 12000 period between 6000 and 18000 years BP (before present). The sea level curve of Bard *et al.* [1996] documenting this rise is given as Fig. 1. Such a rise may be expected to have had a dramatic effect on river deltas.

The effect of sea level rise depends on the tectonic setting. Along uplifting active margins, the rate of sea level rise relative to the margin itself was less than that predicted by the Bard Curve of Fig. 1. Along slowly subsiding passive margins, however, the full brunt of Holocene sea level rise was felt.

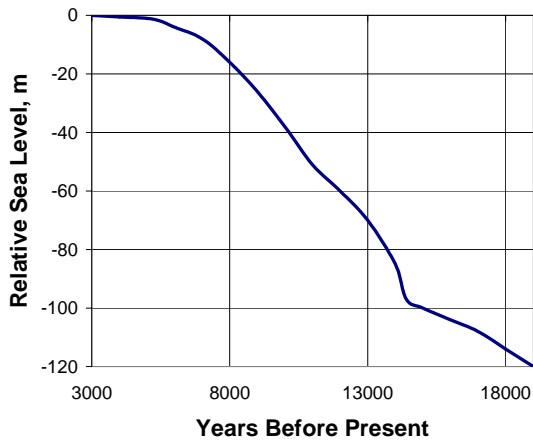


Fig. 1 Sea level curve adapted from Bard et al. [1996].

The passive margin of the East Coast of the US provides an example. The coastline from New Jersey to North Carolina shows a series of embayments, including Delaware Bay, Chesapeake Bay and Albemarle Sound (Fig. 2.) Evidently the mouths of the rivers flowing into this region were drowned by sea level rise. The margin of the northern Gulf of Mexico near the Mississippi River delta, on the other hand, presents a very different picture (Fig. 3). Evidence suggests that the

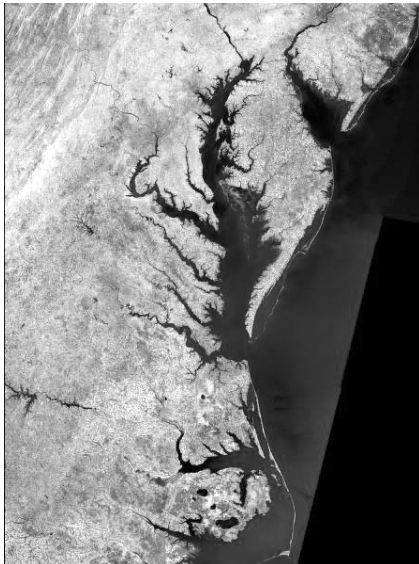


Fig. 2 Coastline of the United States from New Jersey (north) to North Carolina (south).

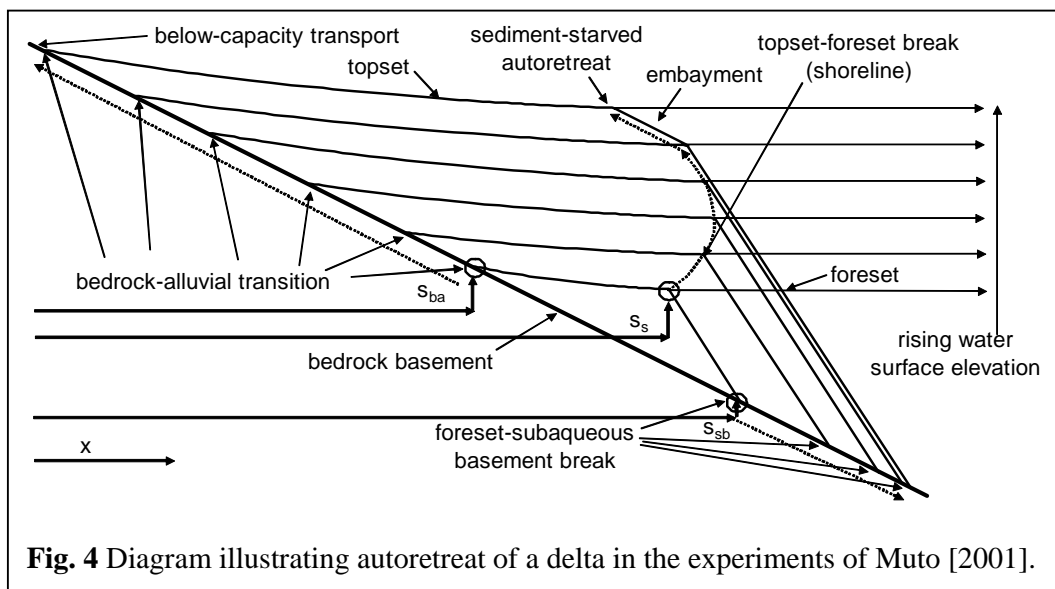


Fig. 3 Coastline of the United States in the vicinity of the delta of the Mississippi River as it flows into the Gulf of Mexico.

Mississippi Delta was able to continue to prograde throughout Holocene sea level rise.

Why would rivers along the same margin of the same continent respond so differently to A key feature is sediment supply.

Holocene sea level rise?



Most of the rivers of Fig. 1 flow from the Appalachian Mountains, a geologically old formation that no longer uplifts and produces little sediment. The Mississippi River, on the other hand, drains a huge area that includes much of the geologically young Rocky Mountains. Evidently under the right conditions a sufficiently high sediment supply can prevent river mouths from being drowned due to sea level rise.

Delta response to sea level rise: autoretreat

The experiments of Muto [2001] offer a direct way to study the effect of sea level rise on river deltas. They were conducted in a narrow channel of constant width, within which a 1D delta was created (Fig. 4). Sediment was fed into a flow over a sloping basement which modeled bedrock. At some point downstream the bedrock basement dropped below a surface of ponded water. The elevation of the ponded water (base level) was raised at a constant rate in time.

Sediment entering flume was transported at below-capacity conditions over the model bedrock channel before reaching an abrupt bedrock-alluvial transition. The alluvial topset had an upward-concave long profile marking the tendency of sediment to deposit on it. A second abrupt transition formed as a topset-foreset break; the subaqueous foreset formed at the angle of repose of the sediment. A third abrupt transition occurred at the break between the foreset and the subaqueous bedrock basement at the toe of the delta.

Under conditions of constant base level the delta always prograded seaward. The shoreline and the foreset toe both moved seaward, and the bedrock-alluvial transition moved landward as the alluvium overlapped onto the bedrock. Under conditions of base level rising at a constant rate, however, the behavior of the delta changed dramatically, as described in Fig. 4. At first the delta shoreline prograded seaward. In time, however, the need to fill an ever-increasing accommodation space created by rising sea level was such that eventually the shoreline began to transgress, or move landward, even though the delta toe continued to move seaward. Finally, at some point the sediment delivery to the shoreline dropped to zero. After this time the subaqueous delta was abandoned and the shoreline began to transgress rapidly, creating a zone of deep water (embayment) behind it.

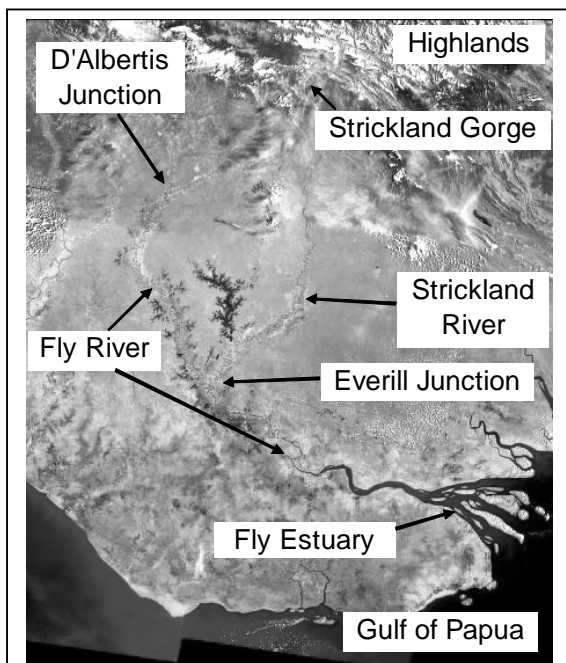


Fig. 5 The Fly-Strickland River System, Papua New Guinea.

Muto and Steel [1992, 1997] called this transgression due to sea level rise “autorettreat.” The process autorettreat begins as soon as the shoreline starts to move landward. As long as sediment is still being delivered to the delta face no embayment is created. If sea level rise is continued for a sufficiently long duration, however, the sediment delivery to the delta face eventually drops to zero, and rapid, sediment-starved autorettreat with the creation of a deep embayment commences.

Muto [2001] developed a geometric model of autorettreat. Whether or not a delta goes into autorettreat depends on sediment supply and the rate and duration of base level rise. For any given rate and duration of rise, the delta goes

into autorettreat for a sufficiently low sediment supply. If base level rise is continued indefinitely, the delta eventually goes into autorettreat regardless of the sediment supply.

The experiments of Muto [2001] allow interpretation of the difference between Figs. 2. and 3. Apparently the sediment supply to the Appalachian-sourced streams in Fig. 2 was not sufficient to prevent autorettreat and delta drowning due to 120 m of sea level rise over 12000 years. The sediment supply to the Mississippi Delta, however, appears to have been sufficient to allow progradation over the same period.

Parker and Muto [2003] have reproduced the experimental results of Muto [2001] using a 1D numerical model of delta morphodynamics. Here this model is adapted to field conditions in order to predict river behavior at field scale.

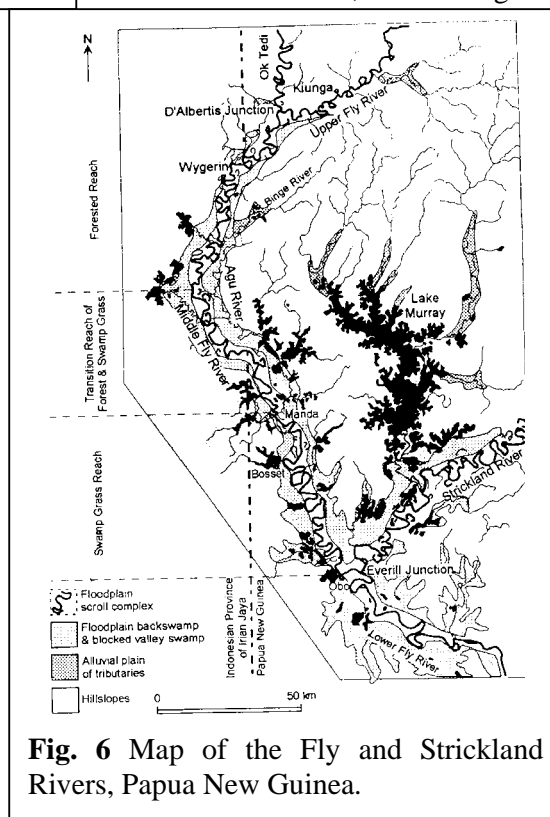


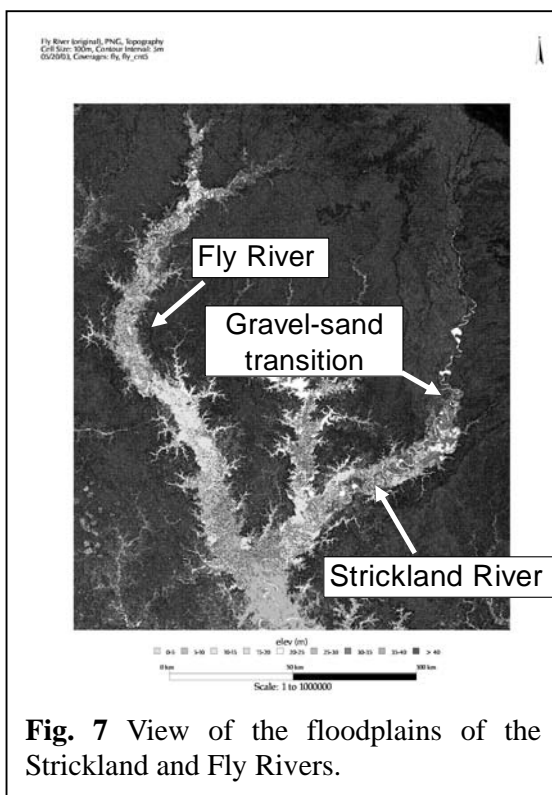
Fig. 6 Map of the Fly and Strickland Rivers, Papua New Guinea.

THE FLY-STRICKLAND RIVER SYSTEM

Overview

The Fly-Strickland River System drains the tectonically active highlands of Papua New Guinea, crosses the Fly Platform and flows into the Gulf of Papua (Fig. 5). The lower Fly River is the reach below Everill Junction (Fig. 5). Everill Junction is formed by the confluence of the middle Fly River from the west and the larger Strickland River from the east (Fig. 5).

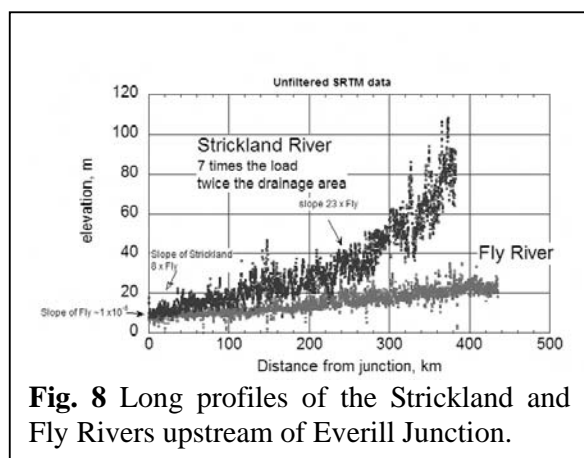
A characteristic feature of the Fly and Strickland Rivers above Everill Junction is the presence of numerous blocked-valley lakes, the largest of which is Lake Murray (Fig. 6). These lakes appear to have formed in response to Holocene sea level rise. That is, sea level rise forced aggradation on the main-stem Fly and Strickland Rivers, both of which have sediment supplies



sourced in the highlands. The small tributaries flowing into the Fly and Strickland Rivers in Fig. 6 are not sourced in the highlands, and as a result have much lower sediment yields per unit drainage area. As a result they were not able to aggrade in pace with main-stem aggradation, so resulting in the blocked-valley lakes (Pickup [1984], Dietrich *et al.* [1999]).

Discharge and long profiles of the Fly-Strickland River System

The Middle Fly River between D'Albertis Junction and Everill Junction has a down-channel length of about 450 km (Figs. 5, 6). A number of smaller tributaries, but no major tributaries enter this reach. As a result the mean annual discharge



increases only from about 1900 m³/s at D'Albertis Junction to about 2500 m³/s at Everill Junction. At present this reach of the river is affected by sediment input from a mine. Under pre-mine conditions, however, it is estimated that the mean annual sediment discharge increased only from 6.9 million tons per year at D'Albertis Junction to 8.0 million tons per year at Everill Junction. The Fly River has a sand bed throughout this reach.

Discharges on the Strickland

River upstream of Everill Junction are less well documented. The mean annual discharge at Everill Junction is on the order of 3500 m³/s. The floodplain of the Strickland River is shown in Fig. 7; a transition from gravel-bed to sand-bed morphology is located about 268 km up-channel from Everill Junction. The Strickland River is estimated to carry an annual load near 70 million tons per year at Everill Junction.

Long profiles of the Strickland and Fly Rivers upstream of Everill Junction are given in Fig. 8. The slope of the Middle Fly between D'Albertis Junction and Everill Junction is $\sim 1 \times 10^{-5}$; the corresponding values for the sand-bed and gravel-bed Strickland River reaches are $\sim 1.0 \times 10^{-4}$ and 3.7×10^{-4} , respectively. The much higher slope of the sand-bed Strickland River as compared to the sand-bed Middle Fly River reflects the much higher (and coarser) sediment load. The Fly River from Everill Junction to the delta, where it flows into the Gulf of Papua, has a down-channel length of about 411 km and an average slope of $\sim 1.5 \times 10^{-5}$.

NUMERICAL MODEL

Exner equation of sediment continuity

Rivers are morphologically active during floods. To capture this in a simple way, the river is assumed to be at bankfull flow for fraction of time I_f , when it is morphologically active; otherwise the river is assumed to be morphologically inactive. As the channel aggrades in response to sea level rise the deposit is spread across the floodplain through migration and avulsion. The following parameters are defined: time t ; down-channel coordinate x ; channel bed elevation η ; total volume bed material load (sand) at bankfull flow Q_{tbf} ; floodplain width B_f ; porosity of bed deposit λ_p ; channel sinuosity Ω ; and fraction of wash load (mud) deposited per unit bed material load (sand) in the channel-floodplain complex Λ . The time-averaged Exner equation of sediment continuity thus takes the form

$$(1 - \lambda_p) \frac{\partial \eta}{\partial t} = -\Omega \frac{I_f (1 + \Lambda)}{B_f} \frac{\partial Q_{\text{tbf}}}{\partial x} \quad (1)$$

Flow and sediment transport

Channel hydraulics at bankfull is flow described in terms of a quasi-steady backwater formulation. Thus where U = flow velocity, H = flow depth, $S = -\partial \eta / \partial x$ = bed slope and C_f is a dimensionless bed friction coefficient,

$$U \frac{dU}{dx} = -g \frac{dH}{dx} + gS - C_f \frac{U^2}{H} \quad (2)$$

The boundary condition on (2) is one of specified elevation of standing water (base level) $\xi_d(t)$. Thus if $x = s_s(t)$ is the position of the topset-foreset break (shoreline),

$$(\eta + H) \Big|_{x=s_s} = \xi_d(t) \quad (3)$$

The case of interest here is that of constant rate of base level rise $\dot{\xi}_d$ (e.g. 10 mm/year). Channel resistance is described in terms of a constant value of C_f .

The case of a sand-bed river is considered here. Sediment mobility is governed by the Shields number τ_{bf}^* of the bankfull flow, which is defined as

$$\tau_{bf}^* = \frac{C_f U^2}{RgD} \quad (4)$$

where R denotes the submerged specific gravity of the sediment (1.65 for quartz) and D denotes the characteristic size of the sand in the river bed. Sand transport is described in terms of the total bed material relation of Engelund and Hansen [1967]; where B denotes the bankfull width of the channel,

$$Q_{tbf} = B\sqrt{RgD} D \frac{0.05}{C_f} (\tau_{bf}^*)^{5/2} \quad (5)$$

Downstream varying bankfull channel geometry

A simple way to describe the bankfull characteristics of a channel is in terms of a specified bankfull Shields number τ_{bf}^* . Parker *et al.* [1998] have found that the following approximate closure is appropriate for sand-bed streams:

$$\tau_{bf}^* = 1.86 \quad (6)$$

Between (5) and (7) the following relation is found for U;

$$\frac{U}{\sqrt{RgD}} = \left(\frac{\tau_{bf}^*}{C_f} \right)^{1/2} \quad (7)$$

Thus for constant values of τ_{bf}^* , C_f , grain size D and sediment submerged specific gravity R, (8) specifies a bankfull flow velocity that remains constant in the downstream direction. Substituting (7) into (2) and reducing,

$$\frac{dH}{dx} = S - R\tau_{bf}^* \frac{D}{H}, \quad S = -\frac{\partial\eta}{\partial x} \quad (8)$$

For a river profile $\eta(x,t)$ at any time t, (8) can be solved subject to (3) to determine the streamwise variation in depth H. It is here assumed that the river has no tributaries over the reach of interest, so that bankfull water discharge Q_{bf} is constant in the streamwise direction. Water continuity requires that

$$Q_{bf} = BUH \quad (9)$$

in which case the streamwise varying bankfull width is given from (6), (7) and (9) as

$$B = \left(\frac{C_f}{\tau_{bf}^*} \right)^{1/2} \frac{Q_w}{\sqrt{RgD} H} \quad (10)$$

Once the streamwise variation of H and B at bankfull flow are computed for a given bed profile, the streamwise variation in total bed material load Q_{tbf} at bankfull flow is computed from (5)

Continuity and shock conditions

In the present analysis the gravel-sand transition of Fig. 7 is replaced with a bedrock-alluvial transition, where the alluvium is sand. This replacement is made for the sake of simplicity; in future work a gravel-sand transition can be included.

The numerical model has three moving boundaries: the position $x = s_{ba}(t)$ of the bedrock-alluvial transition, $x = s_d(t)$ of the delta topset-foreset break and $x = s_{sb}(t)$ of the break between the foreset and the subaqueous basement (Fig. 4). Two continuity conditions must hold: at $x = s_{ba}(t)$ the bedrock elevation must match the alluvial bed elevation, and at $x = s_{sb}(t)$ the foreset elevation must match the subaqueous basement

elevation. In addition, a shock condition for the foreset is obtained by integrating (1) over the foreset. Details concerning the derivation of these conditions are given in Parker and Muto (2003). The results are as follows; where S_{bb} denotes the slope of the bedrock channel upstream of $x = s_{ba}$, S_{sb} denotes the subaqueous bed slope downstream of $x = s_{sb}$, S_{fore} denotes the slope of the foreset face, S_{aba} denotes the alluvial bed slope at $x = s_{ba}$ and S_{ad} denotes the alluvial bed slope at $x = s_d$,

$$(S_{bb} - S_{aba})\dot{s}_{ba} = -\left.\frac{\partial\eta}{\partial t}\right|_{x=s_{ba}}, \quad S_{aba} = -\left.\frac{\partial\eta}{\partial x}\right|_{x=s_{ba}} \quad (11)$$

$$(S_a - S_{sb})\dot{s}_{sb} = (S_{fore} - S_{ad})\dot{s}_d + \left.\frac{\partial\eta}{\partial t}\right|_{x=s_d}, \quad S_{ad} = -\left.\frac{\partial\eta}{\partial x}\right|_{x=s_d} \quad (12)$$

$$(1 - \lambda_p)B_f(s_{sb} - s_d) \left[(S_{fore} - S_{ad})\dot{s}_d + \left.\frac{\partial\eta}{\partial t}\right|_{x=s_d} \right] = I_f(1 + \Lambda)Q_{tbf}|_{x=s_d} \quad (13)$$

The above three relations specify the migration speeds \dot{s}_{ba} , \dot{s}_d and \dot{s}_{sb} of the three transition points of Fig. 4.

Transformation to moving boundary coordinates

In order to include the dynamics of the moving boundaries, the following transformations are introduced;

$$\bar{x} = \frac{x - s_{ba}}{s_d - s_{ba}}, \quad \bar{t} = t \quad (14)$$

The Exner equation (1) thus transforms to

$$(1 - \lambda_p) \left\{ \frac{\partial\eta}{\partial\bar{t}} - \left[\frac{\bar{x}\dot{s}_d + (1 - \bar{x})\dot{s}_{ba}}{s_d - s_{ba}} \right] \frac{\partial\eta}{\partial\bar{x}} \right\} = -\Omega \frac{I_f(1 + \Lambda)}{B_f(s_d - s_{ba})} \frac{\partial Q_{tbf}}{\partial\bar{x}} \quad (15)$$

Equations (11) – (13) are similarly transformed to moving coordinates and reduced with (15) before solving; the results are not shown here for the sake of brevity.

CALCULATIONS

Parameter specification

The Fly-Strickland River System is simplified to a single river with no tributaries and constant bankfull discharge from the gravel-sand transition of Fig. 7 to the Fly Delta. The gravel-sand transition is replaced with a bedrock-alluvial transition. The following values are used based on available data: $Q_{bf} = 4000 \text{ m}^3/\text{s}$, $I_f = 0.35$, $B_f = 8 \text{ km}$, $D = 0.2 \text{ mm}$, $R = 1.65$, $\lambda_p = 0.4$, $\Omega = 2$, $S_{fore} = 0.02$, $S_{bb} = 0.0004$, $S_{sb} = 0.00075$ and $C_f = 0.0025$. The upstream supply of sand is taken to be 14 Mt/a , i.e. 20% of the observed total load (bed material load + wash load) of 70 Mt/a of the Strickland River upstream of Everill Junction. The annual transport is realized in the 35% of the time the river is at bankfull flow. Also $\Lambda = 1.5$, so that for each unit of sand deposited in the channel-floodplain complex 1.5 units of mud is deposited. The reach has an initial length of 650 km and an initial slope of 0.0001 . The initial base of the foreset is set at a datum of 0 m ; the initial foreset top is 30 m above datum, and the initial water surface elevation is 37 m above datum.

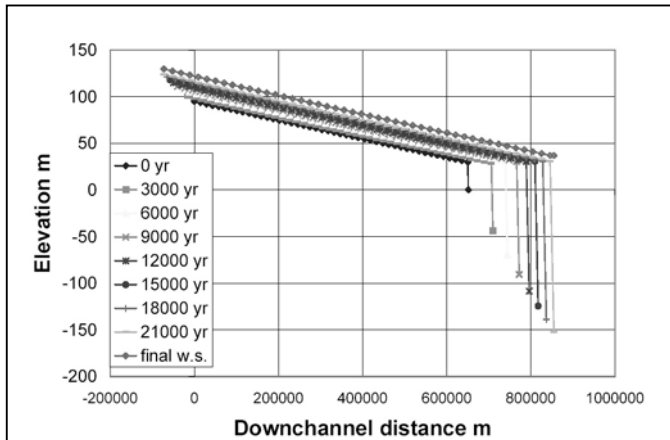


Fig. 9 Case A: constant sea level over 21000 years.

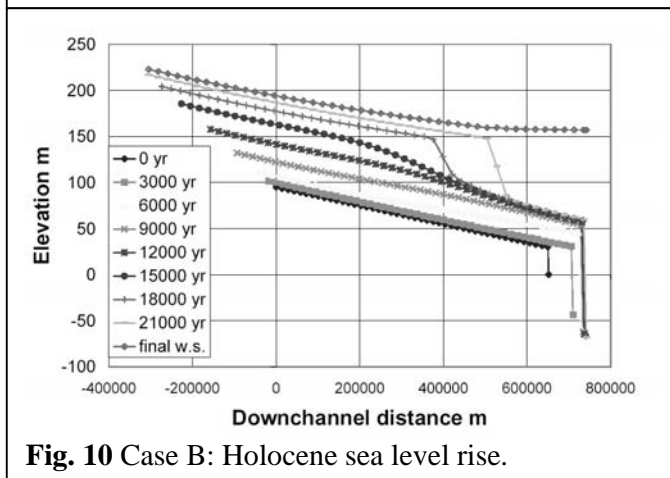


Fig. 10 Case B: Holocene sea level rise.

The calculations are based on the following scenario for Holocene sea level rise. Case A is a reference case in which sea level is held constant at low stand for 21000 years. In Case B, sea level is held constant at low stand for 3000 years. Between 3000 and 15000 years sea level rises at 10 mm/year. Between 15000 and 21000 years sea level is held constant at high stand. The period of sea level rise corresponds to 18000 to 6000 BP; high stand corresponds to 6000 years BP to present.

Results

The results for Cases A and B are shown in Figs. 9 and 10, respectively. Fig. 9 corresponds to constant low-stand sea level; the delta continuously progrades outward and the sand

continuously onlaps onto the bedrock, forcing the bedrock-alluvial transition to move upstream. The river long profile is upward concave, but the concavity is suppressed by the rather steep subaqueous basement slope of 0.00075 over which the delta must prograde.

Fig. 10 shows the case of Holocene sea level rise. The delta continues to prograde up to about 3000 years after the start of sea level rise, but after that it goes into autoretreat. The delta front is abandoned, and a deep embayment forms. The shoreline (as best indicated by the rollover of the long profile as it enters deep water) undergoes transgression, moving some 390 km upstream by the end of sea level rise. During the 6000 years of high stand the delta progrades about 160 km outward. The outward-flaring Fly Estuary evident in Fig. 5 may thus be a relict of autoretreat driven by Holocene sea level rise that has yet to be obliterated by the present high stand. It is seen from Fig. 10 that sea level rise exacerbates the upstream movement of the bedrock-alluvial transition.

CONCLUSION

Implications

The numerical model verifies Muto's [2001] concept of autoretreat at field scale, and quantifies it for the Fly-Strickland River System, Papua New Guinea. The model suggests that Holocene sea level rise likely had a profound effect on both the river delta (drowning it) and the river profile itself (increasing concavity of the long profile and forcing the upstream end of the sand-bed reach landward.

The landward migration of the bedrock-alluvial transition evident in both Figs. 9 and 10 is partly an artifact of the model. This is because the Fly Platform and highlands upstream of the gravel-sand transition in Fig. 7 appear to be undergoing active uplift. Uplift upstream of the transition should slow (but not necessarily stop) its rapid upstream migration under conditions of Holocene sea level rise. An upstream uplifting zone can be included in the model at a later date.

Acknowledgements

This research was funded by a) National Science Foundation grants from the MARGINS program to G. Parker and W. Dietrich, b) the National Center for Earth-surface Dynamics, a National Science Foundation Science and Technology Center, and c) the Japan Association for the Advancement of Science, which funded the postdoctoral studies of Y. Akamatsu.

REFERENCES

- Bard, E., Hamelin, B., Arnold, M., Montaggioni, L., Cabioch, G., Faure, G. and Rougerie, F. (1996) Deglacial sea-level record from Tahiti corals and the timing of global meltwater discharge, *Nature*, 382, pp. 241-244.
- Dietrich, W. E., Day, G. and Parker, G. (1999) The Fly River, Papua New Guinea: inferences about river dynamics, floodplain sedimentation and fate of sediment, In *Varieties of Fluvial Form*, Miller, A. J. and Gupta, A., eds., John Wiley and Sons, New York, pp. 345-376.
- Engelund, F. and Hansen, E. (1967) *A Monograph on Sediment Transport in Alluvial Streams*, Technisk Vorlag, Copenhagen, Denmark.
- Muto, T. (2001) Shoreline autoretreat substantiated in flume experiment, *Journal of Sedimentary Research*, 71(2), pp. 246-254.
- Muto, T. and Steel, R. J. (1992) Retreat of the front in a prograding delta, *Geology*, 20, pp. 967-970.
- Muto, T. and Steel, R. J. (1997) Principles of regression and transgression: the nature of the interplay between accommodation and sediment supply, *Journal of Sedimentary Research*, 67, pp. 994-1000.
- Parker, G., Paola, C., Whipple, K. and Mohrig, D. (1998) Alluvial fans formed by channelized fluvial and sheet flow: theory, *Journal of Hydraulic Engineering*, 124(10), pp. 1-11.
- Parker, G. and Muto, T. (2003) 1D numerical model of delta response to rising sea level, *Proceedings*, 3rd IAHR Symposium, River, Coastal and Estuarine Morphodynamics, Barcelona, Spain, September 1-5., 10 p.
- Pickup, G. (1984) Geomorphology of tropical rivers, I. Landforms, hydrology and sedimentation in the Fly and lower Purari, Papua New Guinea, *Catena Suppl.* 5, pp. 1-17.